

## Structure and energetics of nanotwins in cubic boron nitrides

Shijian Zheng, Rui Feng Zhang, Rong Huang, Takashi Taniguchi, Xiuliang Ma, Yuichi Ikuhara, and Irene J. Beyerlein

Citation: *Applied Physics Letters* **109**, 081901 (2016); doi: 10.1063/1.4961240

View online: <http://dx.doi.org/10.1063/1.4961240>

View Table of Contents: <http://scitation.aip.org/content/aip/journal/apl/109/8?ver=pdfcov>

Published by the [AIP Publishing](#)

---

### Articles you may be interested in

[Structural and electronic properties of cubic boron nitride doped with zinc](#)  
J. Appl. Phys. **116**, 043507 (2014); 10.1063/1.4890607

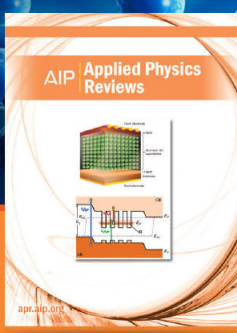
[Weak morphology dependent valence band structure of boron nitride](#)  
J. Appl. Phys. **114**, 054306 (2013); 10.1063/1.4817430

[Oxygen segregation at coherent grain boundaries of cubic boron nitride](#)  
Appl. Phys. Lett. **102**, 091607 (2013); 10.1063/1.4795300

[Structure of boron nitride nanotubules](#)  
Appl. Phys. Lett. **78**, 2772 (2001); 10.1063/1.1367906

[Atomic geometry and energetics of vacancies and antisites in cubic boron nitride](#)  
Appl. Phys. Lett. **74**, 2984 (1999); 10.1063/1.123987

---



**NEW Special Topic Sections**

**NOW ONLINE**  
Lithium Niobate Properties and Applications:  
Reviews of Emerging Trends

**AIP** | Applied Physics Reviews

# Structure and energetics of nanotwins in cubic boron nitrides

Shijian Zheng,<sup>1,a,b)</sup> Ruifang Zhang,<sup>2,a,b)</sup> Rong Huang,<sup>3</sup> Takashi Taniguchi,<sup>4</sup> Xiuliang Ma,<sup>1</sup> Yuichi Ikuhara,<sup>5,6</sup> and Irene J. Beyerlein<sup>7</sup>

<sup>1</sup>Shenyang National Laboratory for Materials Science, Institute of Metal Research, Chinese Academy of Sciences, Shenyang 110016, China

<sup>2</sup>School of Materials Science and Engineering, and International Research Institute for Multidisciplinary Science, Beihang University, Beijing 100191, China

<sup>3</sup>Key Laboratory of Polar Materials and Devices, Ministry of Education, East China Normal University, Shanghai 200062, People's Republic of China

<sup>4</sup>National Institute for Materials Science, Tsukuba, Ibaraki 305-0044, Japan

<sup>5</sup>Nanostructures Research Laboratory, Japan Fine Ceramics Center, Nagoya 456-8587, Japan

<sup>6</sup>Institute of Engineering Innovation, The University of Tokyo, Tokyo 113-8656, Japan

<sup>7</sup>Theoretical Division, Los Alamos National Laboratory, Los Alamos, New Mexico 87545, USA

(Received 5 May 2016; accepted 6 July 2016; published online 22 August 2016)

Recently, nanotwinned cubic boron nitrides (NT c-BN) have demonstrated extraordinary leaps in hardness. However, an understanding of the underlying mechanisms that enable nanotwins to give orders of magnitude increases in material hardness is still lacking. Here, using transmission electron microscopy, we report that the defect density of twin boundaries depends on nanotwin thickness, becoming defect-free, and hence more stable, as it decreases below 5 nm. Using *ab initio* density functional theory calculations, we reveal that the Shockley partials, which may dominate plastic deformation in c-BNs, show a high energetic barrier. We also report that the c-BN twin boundary has an asymmetrically charged electronic structure that would resist migration of the twin boundary under stress. These results provide important insight into possible nanotwin hardening mechanisms in c-BN, as well as how to design these nanostructured materials to reach their full potential in hardness and strength. *Published by AIP Publishing.* [<http://dx.doi.org/10.1063/1.4961240>]

Nanotwinned (NT) metals are an excellent example of how the structure of internal boundaries can greatly influence material strength and hardness.<sup>1–3</sup> These materials are comprised of a high density of coherent twin boundaries (CTBs) spaced tens of nanometers apart ( $10^0$ – $10^2$  nm).<sup>4–6</sup> These boundaries are stable and free of intrinsic defects, such as vacancies and dislocations at grain boundaries (GBs).<sup>7,8</sup> As CTB spacing  $h$  decreases, hardness increases, following the well-known Hall-Petch (HP) relation,  $\sim h^{-1/2}$ .<sup>9</sup> However, at some critical value of  $h$ , the hardness is often observed to plateau or even decrease with further reductions in  $h$  (e.g.,  $\sim 15$  nm for polycrystalline NT copper).<sup>5,10–12</sup> The breakdown in the HP relation is usually related to the nucleation of dislocations from the other two types of boundaries found in NT metals—*incoherent* twin boundaries (ITBs) and grain boundaries (GBs), which contain point defects, dislocations, and disconnections.<sup>13,14</sup> This limited NT spacing  $h$  is unfortunately significantly larger than the theoretical minimum (e.g.,  $\sim 0.6$  nm for copper) and hence the highest possible hardnesses cannot be realized.<sup>15,16</sup>

In contrast to NT metals, a recent NT cubic boron nitride (c-BN) exhibited no such softening in hardness as the twin thickness was reduced to 3.8 nm.<sup>17</sup> It is therefore possible that even higher hardness values can be achieved; nonetheless the actual peak value of hardness has yet to be clarified.<sup>18–20</sup> However, NT c-BN also contains GBs and ITBs arranged in a similar manner as in NT metals. It is, therefore,

puzzling why HP strengthening persisted in NT c-BN, even at such small twin thicknesses.

Here, we provide evidence that plastic deformation in NT c-BN likely involves glide of Shockley partials on CTBs and reveal some unique structural features of these CTBs that make this deformation mechanism highly difficult. As a consequence, NT c-BN would be extraordinarily stable against the mechanical stresses experienced in hardness testing.

Bulk NT c-BN was fabricated via the phase transformation of hexagonal BN (h-BN) powder under a high pressure of 12 GPa and a high temperature of 1973 K.<sup>21</sup> This fabrication process should involve plastic deformation, unlike c-BN fabricated by rapid laser melting and quenching, which did not show deformation defects, such as dislocations and twins.<sup>22</sup> It should be noted that the resulting material does not possess a hardness as high as that reported to date.<sup>17</sup> The difference may be due to a different texture, a larger range of grain sizes ( $10^1$ – $10^3$  nm), and an inhomogeneous distribution of NT regions. Nonetheless, the present c-BN nanostructure is still suitable for revealing the basic, intrinsic features of nanotwins that can contribute to significantly enhanced hardness.<sup>21</sup> In what follows, we use transmission electron microscopy (TEM), scanning transmission electron microscopy (STEM), and *ab initio* density functional theory (DFT) calculations to examine the structures of the dislocations and CTBs in the NT c-BN over a range of electronic, atomic, and nano length scales.

For NT face centered cubic (FCC) metals, it has been argued that the defects, mainly in the form of atomic steps, tend to form in the CTBs as the twin thickness decreases leading to a breakdown in the HP scaling since they can act

<sup>a</sup>Authors to whom correspondence should be addressed. Electronic addresses: sjzheng@imr.ac.cn and zrf@buaa.edu.cn

<sup>b</sup>S. Zheng and R. Zhang contributed equally to this work.

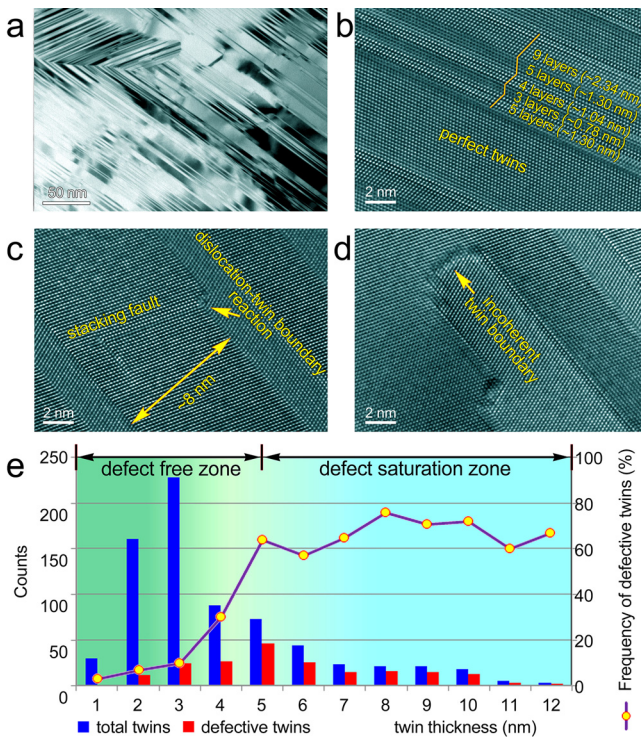


FIG. 1. Nanotwinned structures and twin distribution: (a) morphology of the nanotwins inside c-BN grains, (b) perfect coherent twin boundaries in twins with thicknesses of only few nm, (c) defective twin boundary and (d) incoherent twin boundary in twins with thicknesses of several nm and above, (e) distribution of twins and frequency of defective twins indicating a critical twin thickness of 5 nm below which defects, specifically atomic steps, rarely exist.

as sources for mobile dislocations.<sup>10,23</sup> Using TEM, we examined the defect structure of 650 CTBs and confirmed that the NT c-BN possesses a high density of CTBs and a much lower density of ITBs that terminate within the grains (Fig. 1(a) and also see [supplementary material](#), Fig. S1).<sup>6</sup> Figure 1(e) shows the twin spacing distribution. It is strongly skewed such that many twin boundaries (75%) are spaced 2–4 nm apart and fewer are spaced greater than 5 nm apart, giving an average spacing of 4.2 nm. Most (more than 60%) CTBs associated with twin spacings greater than 5 nm contain many defects, whereas a majority of the CTBs (more than 70%) with spacings less than 5 nm are defect-free

(Fig. 1(b)). Further examination with high-resolution (HR)-TEM reveals that, besides the ITBs (Fig. 1(d)), the defects are predominantly in the form of atomic steps, varying in height and width (Fig. 1(c) and also see [supplementary material](#), Fig. S2). Therefore, contrary to NT metals, CTBs in c-BN are less likely to serve as sources for dislocations as twin spacing decreases below 5 nm since they present significantly less atomic steps. Larger spacings (>5 nm) provide room for a dislocation to nucleate and move, and hence greater opportunity for an interaction with CTBs and for generating defects. Finer spacings (<5 nm), however, do not offer sufficient space. On this basis, the nearly defect-free CTBs associated with the very fine twins ought to lead to high hardness values for NT c-BN.

Understanding the plastic deformation processes during hardness testing requires first uncovering the basic structure of the governing dislocation. Fig. 2(a) shows a dislocation found in this material, which is a glide-set dislocation, spread on the  $\langle 111 \rangle$  plane, which is just one of the types of dislocations possible for the diamond cubic lattice crystal structure of c-BN.<sup>24</sup> To determine whether this type of dislocation dominates, we employ DFT to calculate its stacking fault energy [also see [supplementary material](#) for the methods]. The other class of dislocations in the c-BN diamond cubic lattice is a shuffle-set dislocation.<sup>24</sup> The energy barrier for these dislocations can be expected to be different since the atomic displacements associated with their formation are not the same.<sup>25</sup> Figure 2(b) compares the energy barrier with atomic shifts along the  $\langle 110 \rangle$  direction. The computation shows that the barrier is higher for the glide-set than for the shuffle-set dislocation.

The glide-set dislocations with higher energy barrier, however, can dissociate into two glissile Shockley partials with an intrinsic stacking fault in-between following the same reaction as that for an FCC metal, i.e.,  $a/2[\bar{1}\bar{1}0] \rightarrow a/6[\bar{1}\bar{2}1] + a/6[\bar{2}\bar{1}\bar{1}]$ , as illustrated in Fig. 2(a). A similar dissociation of the shuffle-set dislocations has not been revealed in c-BN. In a similar material, diamond, it has been reported that the most favorable energetic dissociation of the shuffle-set dislocations does not lead to two glissile partials and would require much more energy than the glide-set dissociation

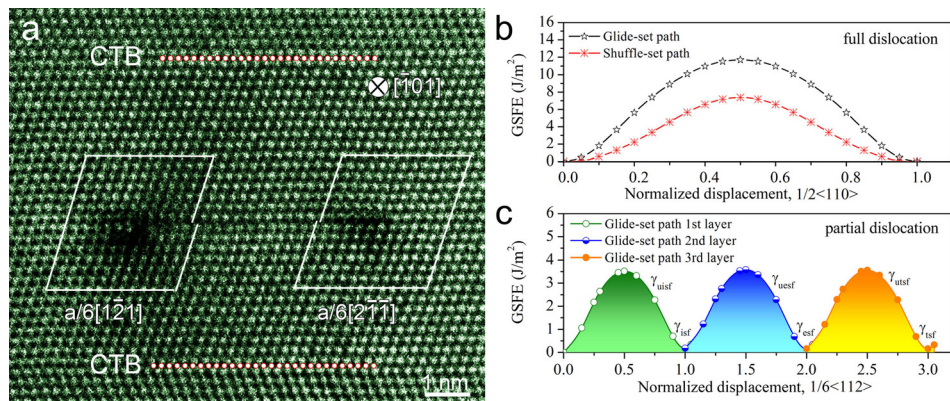


FIG. 2. (a) Dissociation of a glide-set full dislocation into two partials; (b) and (c) the calculated energy profiles with possible dislocation paths: (b) glide-set path and shuffle-set path along the  $\langle 110 \rangle$  direction for full dislocations and (c) the  $\langle 112 \rangle$  direction for partial dislocations. The higher energy barriers for full dislocation path as compared to the partial dislocation path indicate that the preferable paths are partial dislocations.  $\gamma_{uisf}$ : unstable intrinsic stacking fault energy,  $\gamma_{iesf}$ : intrinsic stacking fault energy,  $\gamma_{uesf}$ : unstable extrinsic stacking fault energy,  $\gamma_{esf}$ : extrinsic stacking fault energy,  $\gamma_{utsf}$ : unstable twin stacking fault energy, and  $\gamma_{tsf}$ : twin stacking fault energy.

reactions.<sup>26</sup> Using DFT, we compute the energetic barrier (the unstable stacking fault energy)  $\gamma_{uisf}$  to form the glissile Shockley partial to be  $3.6 \text{ J/m}^2$ , which is substantially lower than that to form either type of full dislocation. The penalty of this intrinsic reaction is the energy associated with forming the stacking fault  $\gamma_{isf}$ , which we calculate to be  $179 \text{ mJ/m}^2$ . The  $\gamma_{isf}$  in c-BN was recently measured to be  $191 \pm 15 \text{ mJ/m}^2$ <sup>27,28</sup> consistent with this calculation. The width of a dissociated glide-set dislocation can be estimated from an energy balance to be  $w = \mu\alpha^2/(24\pi\gamma_I) = 5.5 \text{ nm}$ , for  $\gamma_{isf} = 179 \text{ mJ/m}^2$  and where  $\mu = 58.3 \text{ GPa}$  is the effective shear modulus of c-BN.<sup>29</sup> This value compares well with the STEM observation in Fig. 2(a).

Although these calculations show that the dissociation is favorable, it is not yet evident whether dissociated full (glide-set) dislocations or single Shockley partials prevail during deformation. Movement of a full dislocation can take place via concomitant gliding of a leading Shockley partial and a trailing Shockley partial on the same glide plane. The likelihood of this glide mechanism scales as  $\gamma_{isf}/\gamma_{uisf}$ , with full dislocations preferred over partials for values greater than 0.3.<sup>30</sup> For FCC metals, this ratio can range from 0.1 to 1.<sup>30</sup> According to our calculations, for c-BN, this ratio is notably very low  $\sim 0.05$ . Therefore, we can conclude that the high energy barrier of the undissociated glide-set dislocation and the extremely low  $\gamma_{isf}/\gamma_{uisf}$  ratio indicate that glide of individual Shockley partials ought to predominate plastic deformation in c-BN.

Results in the foregoing section reveal that defect-free nanotwins with thicknesses less than 5 nm prevail in NT c-BN. They suggest that during deformation of such fine NT structures, such as hardness testing, Shockley partial dislocations should dominate, and as NT thicknesses of 5 nm or less do not provide sufficient room for the dislocations to glide non-planar to the CTBs, they likely glide on the CTBs or on  $\{111\}$  planes parallel to them. This basic process could cause CTB migration, which would shrink or expand the nanotwin thickness. However, as we have found via DFT, glide of Shockley partial on CTBs has a high activation barrier, and thus, as a plastic deformation mechanism during hardness testing, it could give rise to outstanding hardness and continued HP strengthening as nanotwin thickness reduces below 5 nm. To uncover some signs of this mechanism, TEM was used on NT c-BN. Figures 3(a)–3(c) show an intrinsic stacking fault, an extrinsic stacking fault, and a twin, respectively. Although these images were not viewed *in-situ* of the same region, it is known that the first fault could develop by glide of a single Shockley partial in a perfect lattice, the second by successive glide of an identical partial on an intrinsic fault, and the third by another partial gliding on the extrinsic fault. Therefore, evidence in Fig. 3 suggests that these stacking faults could have formed during plastic deformation of the NT c-BN, as it happens in FCC metal. It should be mentioned, however, that an alternative mechanism for nanotwin formation could be phase transformation of h-BN to c-BN during fabrication. Nonetheless, when formed during plastic deformation, twins accommodate strain, and when identical Shockley partials glide on adjacent planes, the twin they produce would have an inclined ITB with an angle of about  $70.5^\circ$ . Figure 3(d) indicates that the twins we examined have

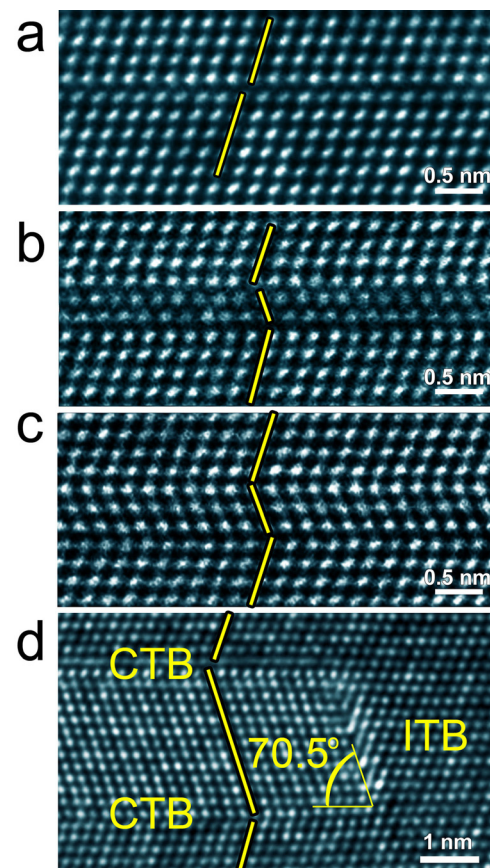


FIG. 3. (a)–(c) Formation mechanism of a twin embryo via the layer-by-layer growth mode of twinning dislocations with identical Burgers vectors: (a) an HAADF-STEM image of an intrinsic stacking fault; (b) an HRTEM image of an extrinsic stacking fault; (c) an HRTEM image of a three-layer twin observed in the nanotwinned samples; (d) a NT giving an angle of about  $70.5^\circ$  between the ITB and CTB.

this feature. On this basis, it appears that Shockley partials glide, along faults or CTBs, is a viable plastic deformation mechanism during hardness testing.

As further support for this observation, we employ DFT to compute the fault energy as a function of the number of fault layers. We find that the fault energy associated with the two-layer fault is  $160 \text{ mJ/m}^2$ , which is lower than that of a monolayer. Similarly, the fault energy of the three-layer stack, i.e., a twin, is  $158 \text{ mJ/m}^2$ , which is also lower than that of a single fault. This calculation suggests that like many FCC metals, a twin that is three-layers thick is favorable and stable.<sup>31</sup> It also implies that twin thicknesses in c-BN could be much finer,  $\sim 0.6 \text{ nm}$ , which is much lower than those reported thus far, and thus much higher hardness could be possible.

Building a 3-layer twin requires the sequential nucleation of Shockley partials on pre-existing faults. As before, the energies required are computed using DFT. For a new Shockley partial on a pre-existing monolayer fault, the energy barrier is  $3.5 \text{ J/m}^2$ , which is smaller than the  $\gamma_{uisf}$  for creating the same partial in a perfect lattice. Repeating the calculation for a Shockley partial on a two-layer stack, we find that the energy is  $3.56 \text{ J/m}^2$ , which again is smaller than  $\gamma_{uisf}$ . These values are over one order of magnitude higher than those in FCC metals,<sup>31</sup> which can be expected since a much higher energy is required to break bonds in c-BN. Prior phase field based mechanics calculations have shown

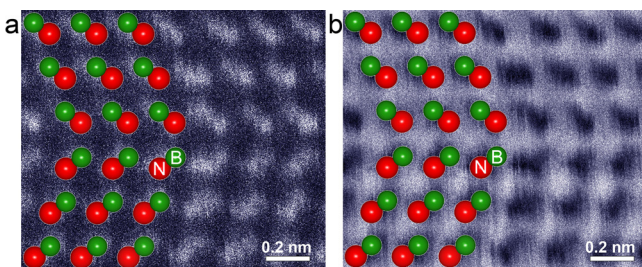


FIG. 4. (a) HAADF-STEM image and (b) ABF-STEM images of the same  $\{111\}$  twin boundary. In the HAADF-STEM image, the heavier N atom columns possess a brighter contrast, while in the ABF-STEM image the heavier N atom columns present a darker contrast.

that the value of  $\gamma_{\text{uisf}}$  scales proportionally with the stresses required to form the twin.<sup>32</sup> Using the model by Joos and Duesbery,<sup>33</sup> a resolved ideal shear strength  $\tau_{\text{max}}$  of 70 GPa can be estimated from the maximum slope of the generalized stacking fault energy (GSFE) curve. Thus, the extremely large energetic barriers to form twinning dislocations in c-BN imply that the formation of a twin in c-BN requires enormously high mechanical stresses. By the same reasoning, it explains why we can expect the hardness of NT c-BN to be exceptionally high. As extreme mechanical forces are required to form twins, similar extreme levels will be needed to de-stabilize them.

The preference for Shockley partial dislocations and the outstanding stability with respect to plastic deformation of the nanotwins they build can be attributed to the one order of magnitude difference (about 20 times) between the high energy to form the partials and low boundary energy of the CTB. In FCC metals, this difference is merely a few times. The low energy of a CTB is partly a consequence of its atomic structure. Here, STEM is used to determine the atomic structure of the CTB in c-BN, with particular attention paid to the B-N bonding across the boundary. Figures 4(a) and 4(b) show the high angle angular dark field (HAADF)-STEM image and corresponding angular bright field (ABF)-STEM image of a CTB in NT c-BN. As expected, the CTB coincides with a  $\{111\}$  plane. However, unlike in FCC metals or NT Diamond, this CTB in c-BN has pseudo-mirror symmetry, with anti-phase symmetry in the B-N bonds at the twin boundaries, which is consistent with a previous report.<sup>34</sup>

In addition to the atomic structure, the fault energies of CTBs are an outcome of the disturbances in charge density associated with the fault. Figure 5 shows the valence charge density difference (VCDD) maps calculated via DFT for the three types of stacking faults, i.e., intrinsic, extrinsic, and twin boundary. The VCDD is defined as the difference between the calculated total valence charge density of the crystal minus the superposition of the valence charge densities of the neutral atoms.<sup>35</sup> A positive value (yellow color) means an increase of the negative charge, while a negative value (cyan color) means a decrease relative to neutral atoms. In these maps, a bigger cyan region means bond weakening by stronger charge depletion. We observe that an asymmetric field is generated at the fault, in which the charge density decreases from the nearest neighbor plane to the fault plane. Around the twin boundary, it is clearly seen that the bigger cyan regions in the VCDD isosurface appear; these are marked by red arrows in Fig. 5 (see supplementary material for a contour plot of VCDD cross section in Fig. S3). Such a discontinuity of charge distribution is unique since  $\text{sp}^3$  hybridization in c-BN provides four ubiquitous equal B-N bonds. The fluctuation in charge density by the introduction of a stacking fault results in the variation of the vertical B-N bond lengths shown in Fig. 5 by italicized numbers. The longest bond length of  $\sim 1.57 \text{ \AA}$  corresponds to the peak charge depletion regions as marked by the red arrows. A similar variation of bond lengths has also been reported previously for the TiN/SiN/TiN heterostructure due to Friedel oscillations at interfaces, which governs its mechanical strength.<sup>36</sup> We also note that this charge redistribution is localized to the region at the fault. These two effects are seen for all three boundary types and can explain the relatively low boundary energy of the CTB. The fact that the bond lengths inside the twins are nearly the same as those within the bulk suggests that significant charge localizations do not induce relatively long-range stress/strain field characteristic of pure metals. This distinction is believed to be responsible for the stability of the unusually high density of finely spaced twins against stress-induced migration. Additionally, the unique asymmetrically charged twin boundary will generate a distinct electronic partition or localization on both sides of the faulted region (unlike in a pure metal), which could further stabilize it against boundary migration and consequently hardness softening.

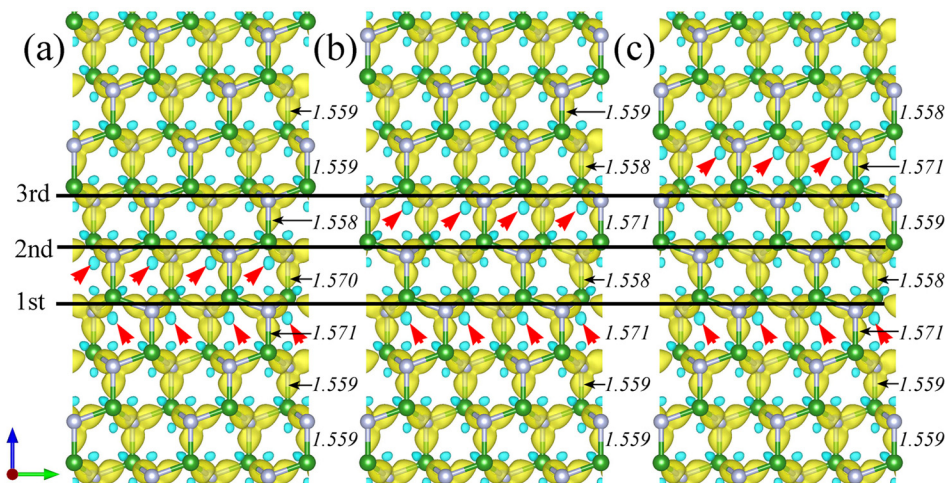


FIG. 5. The calculated isosurfaces of the valence charge density difference (VCDD): (a) an intrinsic stacking fault, (b) an extrinsic stacking fault, and (c) a twin boundary. These indicate strong electronic localization and energetic stability. Blue and yellow regions signify states of charge depletion (negative) and accumulation (positive), respectively. The charge depletion at the fault boundary is distinguished by red arrows. The italicized number shows the lengths of vertical B-N bonds in units of Angstrom.

Taken together, STEM and TEM analyses and *ab initio* DFT calculations of the CTB structure in NT c-BN help to reveal some intrinsic features of nanotwins in c-BN. They not only indicate that plasticity is predominately carried by Shockley partial dislocations but that these partials are exceedingly difficult to nucleate (being  $3.6 \text{ J/m}^2$ ) compared to those in FCC metals. Furthermore, as  $h$  decreases below 5 nm, we find that the CTBs become even less defective, removing the possibility for them to serve as sources for new dislocations. Thus, for plastic deformation in such fine NT c-BN, it is likely that these dislocations are not gliding on (111) planes inclined to the CTBs but rather on the CTBs. In FCC metals, this mechanism is known to cause softening.<sup>10,13,14,23</sup> However, in c-BN, as we show, the energy barriers associated with this mechanism are over one order of magnitude higher than those in FCC metals.<sup>31</sup> Thus, the extraordinary hardness of the NT c-BN CTBs could be attributed to a high resistance to this plastic deformation mechanism. The origin of the unusually high-energy barrier may be related to the electronic structure of the CTBs, which we find exhibit an anti-phase atomic configuration and asymmetric charge density.

See [supplementary material](#) for experimental and simulation details, as well as additional images of defective twin boundaries.

S.J.Z. wishes to acknowledge support from the “Hundred Talents Project” of the Chinese Academy of Sciences and the National Thousand Young Talents Program of China. R.F.Z. is supported by the Fundamental Research Funds for the Central Universities, National Natural Science Foundation of China (51471018), and the National Thousand Young Talents Program of China. I.J.B. would like to acknowledge support from a Laboratory Directed Research and Development Program Award, No. 20140348ER. We would like to thank Professor Dr. S. Veprek for constructive comments and suggestions. We also gratefully acknowledge the support from the National Supercomputer Center at TianJin.

- <sup>1</sup>L. Lu, Y. F. Shen, X. H. Chen, L. H. Qian, and K. Lu, *Science* **304**, 422 (2004).
- <sup>2</sup>K. Lu, L. Lu, and S. Suresh, *Science* **324**, 349 (2009).
- <sup>3</sup>X. Zhang, A. Misra, H. Wang, M. Nastasi, J. D. Embury, T. E. Mitchell, R. G. Hoagland, and J. P. Hirth, *Appl. Phys. Lett.* **84**, 1096 (2004).
- <sup>4</sup>S. J. Zheng, I. J. Beyerlein, J. S. Carpenter, K. Kang, J. Wang, W. Z. Han, and N. A. Mara, *Nat. Commun.* **4**, 1696 (2013).

- <sup>5</sup>I. J. Beyerlein, X. Zhang, and A. Misra, *Annu. Rev. Mater. Res.* **44**, 329 (2014).
- <sup>6</sup>Y. T. Zhu, X. Z. Liao, and X. L. Wu, *Prog. Mater. Sci.* **57**, 1 (2012).
- <sup>7</sup>F. Ernst, M. W. Finnis, A. Koch, C. Schmidt, B. Straumal, and W. Gust, *Zeitschrift Metallkd.* **87**(11), 911–922 (1996).
- <sup>8</sup>O. Anderoglu, A. Misra, H. Wang, and X. Zhang, *J. Appl. Phys.* **103**, 094322 (2008).
- <sup>9</sup>Y. F. Shen, L. Lu, Q. H. Lu, Z. H. Jin, and K. Lu, *Scr. Mater.* **52**, 989 (2005).
- <sup>10</sup>L. Lu, X. Chen, X. Huang, and K. Lu, *Science* **323**, 607 (2009).
- <sup>11</sup>A. Misra, J. P. Hirth, and R. G. Hoagland, *Acta Mater.* **53**, 4817 (2005).
- <sup>12</sup>H. Bahmanpour, K. M. Youssef, J. Horky, D. Setman, M. A. Atwater, M. J. Zehetbauer, R. O. Scattergood, and C. C. Koch, *Acta Mater.* **60**, 3340 (2012).
- <sup>13</sup>X. Y. Li, Y. J. Wei, L. Lu, K. Lu, and H. J. Gao, *Nature* **464**, 877 (2010).
- <sup>14</sup>J. Wang, N. Li, O. Anderoglu, X. Zhang, A. Misra, J. Y. Huang, and J. P. Hirth, *Acta Mater.* **58**, 2262 (2010).
- <sup>15</sup>D. C. Jang, X. Y. Li, H. J. Gao, and J. R. Greer, *Nat. Nanotechnol.* **7**, 594 (2012).
- <sup>16</sup>J. W. Wang, F. Sansoz, J. Y. Huang, Y. Liu, S. H. Sun, Z. Zhang, and S. X. Mao, *Nat. Commun.* **4**, 2768 (2013).
- <sup>17</sup>Y. J. Tian, B. Xu, D. L. Yu, Y. M. Ma, Y. B. Wang, Y. B. Jiang, W. T. Hu, C. C. Tang, Y. F. Gao, K. Luo, Z. S. Zhao, L. M. Wang, B. Wen, J. L. He, and Z. Y. Liu, *Nature* **493**, 385 (2013).
- <sup>18</sup>H. Sumiya, Y. Ishida, K. Arimoto, and K. Harano, *Diamond Relat. Mater.* **48**, 47 (2014).
- <sup>19</sup>A. Nagakubo, H. Ogi, H. Sumiya, and M. Hirao, *Appl. Phys. Lett.* **105**, 081906 (2014).
- <sup>20</sup>B. Li, H. Sun, and C. F. Chen, *Nat. Commun.* **5**, 5965 (2014).
- <sup>21</sup>C. L. Chen, R. Huang, Z. C. Wang, N. Shibata, T. Taniguchi, and Y. Ikuhara, *Diamond Relat. Mater.* **32**, 27 (2013).
- <sup>22</sup>J. Narayan, A. Bhaumik, and W. Xu, *J. Appl. Phys.* **119**, 185302 (2016).
- <sup>23</sup>Y. M. Wang, F. Sansoz, T. LaGrange, R. T. Ott, J. Marian, T. W. Barbee, and A. V. Hamza, *Nat. Mater.* **12**, 697 (2013).
- <sup>24</sup>J. P. Hirth and J. Lothe, *Theory of Dislocations* (Krieger Publishing Company, 1982).
- <sup>25</sup>W. Cai, V. V. Bulatov, J. P. Chang, J. Li, and S. Yip, “Dislocation core effects on mobility,” in *Dislocations in Solids*, edited by F. R. N. Nabarro and J. P. Hirth (Elsevier Science Bv., Amsterdam, 2004), Vol. 12, pp. 1–80.
- <sup>26</sup>A. T. Blumenau, M. I. Heggie, C. J. Fall, R. Jones, and T. Frauenheim, *Phys. Rev. B* **65**, 205205 (2002).
- <sup>27</sup>L. C. Nistor, G. Van Tendeloo, and G. Dinca, *Phys. Status Solidi A* **201**, 2578 (2004).
- <sup>28</sup>L. Nistor, S. Nistor, C. Dinca, J. van Landuyt, D. Schoemaker, V. Copaciu, P. Georgeoni, and N. Arnici, *Diamond Relat. Mater.* **8**, 738 (1999).
- <sup>29</sup>R. F. Zhang, S. Veprek, and A. S. Argon, *Appl. Phys. Lett.* **91**, 201914 (2007).
- <sup>30</sup>N. Bernstein and E. B. Tadmor, *Phys. Rev. B* **69**, 094116 (2004).
- <sup>31</sup>S. Ogata, J. Li, and S. Yip, *Phys. Rev. B* **71**, 224102 (2005).
- <sup>32</sup>A. Hunter and I. J. Beyerlein, *Acta Mater.* **88**, 207 (2015).
- <sup>33</sup>B. Joos and M. S. Duesbery, *Phys. Rev. Lett.* **78**, 266 (1997).
- <sup>34</sup>C. L. Chen, S. H. Lv, Z. C. Wang, M. Saito, N. Shibata, T. Taniguchi, and Y. Ikuhara, *Appl. Phys. Lett.* **102**, 091607 (2013).
- <sup>35</sup>R. F. Zhang, D. Legut, X. D. Wen, S. Veprek, K. Rajan, T. Lookman, H. K. Mao, and Y. S. Zhao, *Phys. Rev. B* **90**, 094115 (2014).
- <sup>36</sup>N. Li, M. S. Martin, O. Anderoglu, A. Misra, L. Shao, H. Wang, and X. Zhang, *J. Appl. Phys.* **105**, 123522 (2009).